Available online at www.sciencedirect.com
SCIENCE DIRECT®
ELSEVIER
Organic Geochemistry 34 (2003) 1635–1650
Organic Geochemistry
www.elsevier.com/locate/orggeochem

^{15}N-CPMAS nuclear magnetic resonance spectroscopy and biological stability of soil organic nitrogen in whole soil and particle-size fractions

R.J. DiCosty[a,*], D.P. Weliky[b], S.J. Anderson[c], E.A. Paul[d]

[a]*USDA Forest Service, Southern Research Station, 320 Green St., Athens, GA 30602, USA*
[b]*Department of Chemistry, Michigan State University, East Lansing, MI 48824, USA*
[c]*Earth Systems Science and Policy, California State University- Monterey Bay, Seaside, CA 93955, USA*
[d]*843 Rossum Dr., Loveland, CO 80537, USA*

Received 20 February 2003; accepted 8 August 2003
(returned to author for revision 10 June 2003)

Abstract

Soil organic nitrogen was quantified by solid-state ^{15}N cross-polarization nuclear magnetic resonance spectroscopy (NMR) during a 14-month laboratory incubation of a sandy loam soil amended with ^{15}N-clover. In whole soil and particle-size fractions, the clover-derived N was always 85–90% amide, 5–10% guanidinium N of arginine, and 5% amino. Quantitativeness of these results was suggested by (1) analysis of a standard containing a complex mixture of organic ^{15}N and (2) correlation of spectral intensities with ^{15}N concentrations. Based on the unchanging proteinaceous NMR signature of clover-derived N throughout the incubation, differences in the mineralization/immobilization kinetics of clover-N among the different particle-size fractions appeared not to be linked to organic functional group. Kinetic analysis of the mineralization of ^{15}N, with correction of rate constants for field temperatures, suggested that the proteinaceous ^{15}N in the clay and fine silt fractions observed here had a mean residence time of 7 years in the field.
© 2003 Elsevier Ltd. All rights reserved.

1. Introduction

The chemical structure of soil organic nitrogen (SON) is controversial. Broadly speaking, soil organic nitrogen has been studied by one of three methods: (1) wet chemical extraction, (2) pyrolysis mass spectrometry, and (3) ^{15}N-nuclear magnetic resonance spectroscopy. Fractions isolated by wet chemical extraction include amino acid-N, amino sugar-N, "NH_3–N",[1] hydrolyzable unknown N, and acid-insoluble N (Stevenson, 1994); about one half of soil N is unidentifiable by this technique (Schnitzer, 1985; Stevenson, 1994). Soil scientists have applied cross-polarization magic-angle spinning ^{15}N-nuclear magnetic resonance spectroscopy in the solid state (CPMAS–NMR) and pyrolysis-mass spectrometry (PyMS) to gain further information about the chemical structure of soil organic N, but the conclusions of different investigators are often contradictory.

Based on PyMS and chromatography studies of whole soils and hydrolysis fractions, Schulten and Schnitzer (1998) state that soil N is distributed as follows: proteins + peptides + amino acids, 40%; amino sugars, 5–6%; heterocyclic N, 35%; and "NH_3", 19%. In a PyMS study of agricultural soils, Schulten and Hempfling (1992) found a negative correlation between heterocyclic N and total soil N. According to these authors, the low-N soils had a decreased capacity to immobilize N (as a result of management practices) and thereby became enriched with relatively resistant heterocyclic N.

* Corresponding author. Fax: +706-559-4317.
E-mail address: rdicosty@fs.fed.us (R.J. DiCosty).

[1] NH_3–N is operationally defined as the ammonia recovered upon steam distillation of MgO-treated hydrolysate.

0146-6380/$ - see front matter © 2003 Elsevier Ltd. All rights reserved.
doi:10.1016/j.orggeochem.2003.08.005

In contrast to the above studies, NMR researchers have found 80% or more of soil N in amide form (peptide bonds in proteins), with the remainder in the form of amino acids, amino sugars, or the amino groups of nucleic acid bases (Knicker et al., 1993, 1997, 1999; Clinton et al., 1995; Hopkins et al., 1997). Heterocyclic N has been identified by NMR analysis of soil humic and fulvic acids, but with concentrations ranging from 4 to 9% (Zhuo and Wen, 1992) or from 9 to 22% (Mahieu et al., 2000). These concentrations of heterocyclic N are below those proposed by Schulten and Schnitzer (1998), and may be somewhat overestimated due to overlap of the relatively small heterocyclic N peaks by the adjacent large amide peak. [See spectra in Zhuo and Wen (1992) and Mahieu et al. (2000).] Given that Schulten and Hempfling (1992) proposed that heterocyclic N is an indicator of agricultural management practices (see above), it is important to reconcile the controversy concerning the chemical nature of soil organic N.

Both PyMS and CPMAS–NMR have potential problems in quantitation of soil organic N. In the case of PyMS, incomplete sample volatilization or thermal rearrangement may confound the analysis (Schulten et al., 1995). In CPMAS–NMR, quantitation may fail if differential relaxation effects during the contact and delay times are not considered. These effects have been assessed in plant material, compost, and soluble extracts (Knicker and Lüdemann, 1995; Knicker et al., 1997), but have not been thoroughly investigated in soil. Another potential problem of CPMAS–NMR is that rigid aromatic structures may have excessively long T_{1H} values (50 s or more) (Wilson et al., 1984); the delay times required to detect the N in such structures may be too lengthy for a practical experiment. Furthermore, NMR studies of soil N often require addition of ^{15}N; incubation time of the ^{15}N with soil may be insufficient for formation of heterocyclic N (Schulten and Schnitzer, 1998). Finally, NMR may be currently unable to detect the numerous heterocyclic N structures thought to be present in soil (Schulten and Schnitzer, 1998). The structures may be obscured by the high frequency shoulder of the amide-N peak. If numerous heterocyclic N structures exist in soil and have a wide range of chemical shifts, the structures may give rise to numerous small signals that are undetectable in a typical CPMAS–NMR experiment.

Despite the limitations of CPMAS–NMR, its non-invasiveness makes it attractive for studies of SON. The technique has only recently been applied to soil particle-size fractions (Knicker et al., 1999), which are known to contain biologically and chemically distinct pools of organic matter (e.g. Catroux and Schnitzer, 1987). It is of interest to determine if the amide-dominated spectra found in the particle-size fractions studied by Knicker et al. (1999) are characteristic of most soils.

Our objectives were to (1) measure differential relaxation effects of the various SON functional groups in a soil amended with ^{15}N clover, (2) test whether CPMAS–NMR is quantitative for both heterocyclic and noncyclic SON, and (3) use CPMAS–NMR to quantify the SON functional groups formed in whole soil and particle-size fractions during clover decomposition.

2. Materials and methods

2.1. Clover-uracil-soil test sample

For testing whether NMR was quantitative (Objectives 1 and 2 of the Introduction), an intimate mixture of ^{15}N-uracil, ^{15}N-clover, and unlabeled soil (Marlette series, see below) was prepared such that the molecular interactions (e.g. binding to soil particles) would be somewhat similar to those expected in a natural soil. The uracil, clover, and soil were combined in a sufficient volume of water for complete dissolution of the uracil; the resulting suspension was mechanically shaken for 1 h, quickly frozen in liquid nitrogen (to minimize precipitation of relatively insoluble uracil), and lyophilized. This mixing method influenced the NMR behavior of the sample; the sample prepared as above exhibited a lower T_{1H} value than a sample mixed only by grinding with mortar and pestle (data not shown). This is likely due to shorter distances between ^{15}N nuclei and paramagnetic species (e.g. Fe) in the water-treated sample. The quantitativeness of NMR for the aforementioned mixture of ^{15}N-uracil, ^{15}N-clover, and unlabeled soil was evaluated by comparing the NMR peak area proportions to the known sample composition, after correction for differential relaxation effects (as described below).

2.2. Soil incubation experiment

2.2.1. Overview

The objective of quantifying soil organic N during clover decomposition (Objective 3 of the Introduction) was addressed via a soil incubation experiment. The Ap horizon of an agricultural soil was amended with ^{15}N-labeled red clover (*Trifolium pratense* L.) and incubated in laboratory microlysimeters for 14 months. Inorganic N was removed via in situ leaching several times during the incubation. On five dates, the incubated soil was ultrasonically fractionated into five size classes, and the concentrations of N and ^{15}N were determined for each size fraction and whole soil. The applicability of the observed N dynamics to field conditions was evaluated by comparing the whole-soil N retention observed here to that measured in the field by other researchers, after making temperature corrections with the Q_{10} equation (Kätterer et al., 1998). On three of the five dates, the

SON in the fractions and whole soil was characterized by CPMAS–NMR.

2.2.2. C, N, and ^{15}N analyses

Total C and N contents of clover, soils, and particle-size fractions were determined by dry combustion (Carlo Erba NA 1500 Series 2 N/C/S Analyzer). The ^{15}N concentrations of the clover, soils and particle-size fractions were determined by mass spectrometry at either Michigan State University (Europa Scientific 20-20 Stable Isotope Analyzer) or University of Georgia. Samples were diluted as necessary with natural abundance N in the form of atropine, soil, or aqueous ammonium sulfate to avoid introducing excessive ^{15}N into the mass spectrometers. For whole soil samples with high levels of nitrate, inorganic N was removed prior to dry combustion and mass spectrometric analyses by thrice extracting with 0.01 M $CaCl_2$. Dixon's gap test (Bliss, 1967) was used to identify outliers at the 10% probability level for replicated elemental and isotopic analyses (C, N and ^{15}N). These outliers comprised a small proportion of the data, and were excluded from the final data due only to their extreme deviations. This was deemed necessary because it is difficult to completely avoid analytical errors in samples with low masses or low concentrations of analytes.

2.2.3. Soil and plant material. The soil used for the incubation was a fine-loamy, mixed mesic Glossoboric Hapludalf (Marlette series) from East Lansing, Michigan, USA. The Ap layer of soil was excavated from 0 to 10 cm depth, air-dried, sieved to remove fragments >2 mm in diameter, and thoroughly mixed.

The particle-size distribution of the soil was determined by the pipet method (Gee and Bauder, 1986; Whittig and Allardice, 1986). Carbonates were removed and the soil cation exchange sites were saturated with sodium by treatment with 1 M sodium acetate (adjusted to pH 5), at 70–80 °C. Excess salts were then removed by centrifugation with water, after which organic matter was removed by addition of 30% hydrogen peroxide at 70 °C. Next, sodium hexametaphosphate was added followed by either 24 h or more of soaking or about 16 h of shaking; both methods gave the same results. Sand (>53 μm diameter) was determined by sieving, and fine silt (2–10 μm) and coarse clay (0.2–2 μm) were determined by shaking the remaining suspension and taking pipet aliquots at the appropriate settling times. Fine clay (<0.2 μm) was determined in a tube centrifuge based on an integrated version of Stokes' law, and coarse silt (10–53 μm) was determined by difference. Throughout the procedure, the presence of residual salts was taken into account by appropriate measurements and corrections. The results are shown in the leftmost data column of Table 1. The soil was identified as a sandy loam per the USDA textural classification system (Brady, 1990).

The clover (*Trifolium pratense* L.) used as a soil amendment had been grown hydroponically using $^{15}NO_3$ as the sole N source. The clover was freeze-dried and ball-milled to a powdery texture prior to mixing it with soil. The characteristics of the clover were as follows (means ± sample standard deviations): N_{total} (g kg^{-1}) = 38.9 ± 1.0, molar C:N ratio = 12.9 ± 0.4, atom% ^{15}N = 91.8 ± 2.0.

2.2.4. Incubation conditions. Soils were incubated at room temperature (about 23 °C) in the dark in laboratory-scale microlysimeters (Nadelhoffer, 1990). Before incubation, the soil was amended with 34.3 g of the ^{15}N-labeled red clover per kg amended soil (dry basis). The total C and N contents of the soil were approximately doubled as a result of adding the amendment, and the clover-C corresponded to about 1.4% of the soil dry weight. The high concentration of clover in the soil ensured that ^{15}N-NMR spectra could be obtained in a reasonable amount of time.

Into each microlysimeter, 62.1 g of amended soil (dry basis) were packed at an approximate bulk density of 1.2 Mg m^{-3}. Then, water was added to −33 kPa soil water potential. The soil water potential was maintained by adding water about twice per week. Excess inorganic N produced by the mineralization of the clover was removed by leaching the microlysimeters on several occasions with N-free nutrient solution (Nadelhoffer, 1990). The N-free nutrient solution contained 1.3 mM $CaCl_2$, 0.67 mM KH_2PO_4, 0.33 mM K_2SO_4, 0.33 mM $MgSO_4$, 8.33 μM H_3BO_3, 0.67 μM $MnCl_2$, 0.67 μM $ZnSO_4$, 0.17 μM $CuSO_4$, and 0.17 μM Na_2MoO_4, with final pH = 5.1. At the end of the study, about 11 pore volumes of leachate had been collected from each microlysimeter.

2.2.5. Ultrasonic fractionation of soil. After 11, 34, 95, 190, and 439 days of incubation, the soil from two microlysimeters was composited, sonicated, and separated into five organo-mineral size classes. The size classes were fine clay (0–0.2 μm diameter), coarse clay (0.2–2 μm), fine silt (2–10 μm), coarse silt (10–53 μm), and sand (53–2000 μm). An ultrasonic energy of 38.3 kJ per 28 g soil was used; the energy was measured as described by Morra et al. (1991) and North (1976). This energy produced a particle-size distribution that was lower in fine clay but higher in coarse clay and fine silt than that of the pipet method (Table 1). Sonication was carried out in a 250-ml beaker that was resting in an ice bath, with a 1:5 soil:water ratio (w/w), 28 g soil (dry basis), 1.27 cm (0.5 in) ultrasonic probe diameter, and 3 cm probe depth. The incubated soils required brief hand-shaking after addition of water; the shaking served to break up large clods of moist soil prior to sonication.

After sonication, the three finest size fractions were physically separated on the basis of Stokes' law. The

Table 1
Particle-size distribution as determined by conventional pipet or ultrasound methods

Fraction	Method		
	Conventional pipet (%)[a]	Ultrasound (38.3 kJ/28 g soil) (%)[a]	Ultrasonic yield/ conventional yield
fine clay (<0.2 μm)	6.5 (0.3)	3.8 (0.6)	0.59
Coarse clay (0.2–2μm)	9.1 (0.9)	12.4 (0.7)	1.37
Fine silt (2–10 μm)	9.9 (0.9)	12.0 (0.4)	1.21
Coarse silt (10–53 μm)	19.7 (0.2)	15.4 (2.9)	0.78
Sand (53–2000 μm)	54.8 (0.2)	56.3 (3.1)	1.03

[a] Sample standard deviations in parentheses.

fine clay was isolated by centrifugation, the coarse clay by gravity sedimentation at 4 °C (the low temperature served to slow microbial transformations), and the fine silt by gravity sedimentation at room temperature. Each separation consisted of eight centrifugation or sedimentation cycles. During the separations, the concentration of clay was kept below 10 g/l because clay concentrations above 10 g/l significantly increase the suspension viscosity relative to pure water and thereby confound the Stokes' law calculations (Elonen, 1971). After the three finest size fractions were isolated, the coarse silt and sand were separated by wet sieving.

When the separations were completed, the three fine size fractions were concentrated by flocculation with $MgCl_2$; the supernatant was removed by siphoning, with centrifugation as necessary. The two coarse size fractions were either flocculated as above or allowed to settle under gravity, and were concentrated by siphoning the supernatant. Salts were removed by dialysis at 4 °C. The separation, concentration, and dialysis were completed in about 2 weeks, with samples stored at 4 °C between steps. The separated fractions and a sample of unfractionated whole soil were lyophilized, and stored at −70 °C.

2.3. NMR spectroscopy

NMR spectra of the solid state samples were acquired on a Varian VXR 400 MHz spectrometer with a frequency of 40.5 MHz for ^{15}N and 400.0 MHz for ^{1}H. Cross-polarization magic-angle spinning (CPMAS) was used to enhance the signal-to-noise ratio and hasten data acquisition (Fig. 1). In the CPMAS technique, a 90° pulse to ^{1}H is followed by a simultaneous irradiation of ^{1}H and ^{15}N at fields corresponding to the Hartmann–Hahn match (Stejskal and Memory, 1994). During this period of simultaneous irradiation (known as the *contact time*), magnetization is transferred from ^{1}H to ^{15}N. The exponential rates of magnetization buildup and decay for ^{15}N during the contact time are characterized by the cross-polarization buildup time (T_{NH}) and spin-lattice relaxation time in the rotating frame ($T_{1\rho H}$), respectively, and vary according to N functional group.

After the contact time, the ^{15}N signal is acquired during a period of high-power proton decoupling (the *acquisition time*). The CPMAS scan then concludes with the delay time, in which the ^{1}H nuclei return (in whole or in part) to equilibrium. The characteristic time T_{1H} for ^{1}H to return to equilibrium (spin-lattice relaxation time of ^{1}H in the laboratory frame) may vary with functional group.

Standard samples were run to ensure optimal performance of the spectrometer before each series of NMR experiments. The magic angle was optimized using KBr. The 90° ^{1}H pulse length, and cross-polarization and decoupling fields were optimized on a setup sample comprised of ^{15}N-uracil, $(^{15}NH_4)_2SO_4$, and unlabeled

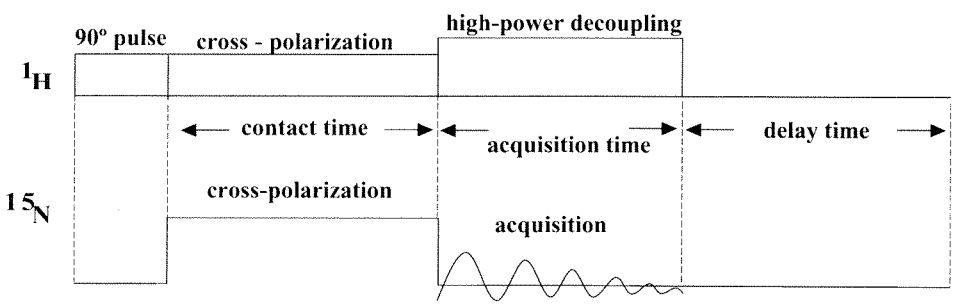

Fig. 1. The cross-polarization magic angle spinning pulse sequence for ^{15}N.

soil. This sample had been intimately mixed in the same manner as was the (uracil + clover + soil) used for testing the quantitativeness of NMR (see above). In the setup sample, the uracil (Fig. 2) served to verify that the spectrometer could detect heterocyclic N, and the narrow resonance of $(^{15}NH_4)_2SO_4$ allowed for precise determination of the cross-polarization fields. The 90° ^1H pulse lengths were between 6.5 and 10.5 μs, and the decoupling frequency during acquisition was 65–80 kHz (as measured with an oscilloscope). With this decoupling frequency and 10 Hz of line broadening, maximum (full-width at half-maximum) linewidths were 4–6 ppm for uracil and 2 ppm for ammonium sulfate. Optimal contact times were 0.2–0.4 ms; delay times were 0.5 s or longer to avoid probe overheating, and acquisition times were 6–10 ms.

For experimental soil samples, 200–300 mg of soil were packed into a silicon nitride rotor of 7 mm diameter and spun at a frequency of 4500 Hz. Chemical shifts were referenced to $(^{15}NH_4)_2SO_4$ (= 0 ppm); chemical shift assignments are summarized in Table 2 and given in detail in Appendix A.

2.3.1. Correction for differential relaxation effects. Differential relaxation effects were considered to insure accurate quantitation of NMR spectra. The following model accounted for differential relaxation effects during the contact and delay times, and is based on concepts and equations presented by Stejskal and Memory (1994):

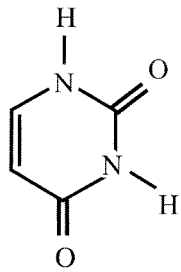

Fig. 2. Chemical structure of uracil.

$$S_0 = S(t_C, t_D)\left[\times \left(\frac{1-(T_{NH}/T_{1\rho H})}{\exp(-t_C/T_{1\rho H}) - \exp(-t_C/T_{NH})}\right) \times \left(\frac{1}{1-\exp(-t_D/T_{1H})}\right)\right] \quad (1)$$

where S_0 is the theoretical signal intensity, $S(t_C,t_D)$ is the measured signal intensity at contact time t_C and delay time t_D, and T_{NH}, $T_{1\rho H}$, and T_{1H} are as described previously. The first and second terms within the square brackets account for differential relaxation during the contact and delay times, respectively. For convenience, the first term within the square brackets will be referred to as the contact-time correction factor (CF_{tC}):

$$CF_{tC} = \frac{1-(T_{NH}/T_{1\rho H})}{\exp(-t_c/T_{1\rho H}) - \exp(-t_c/T_{NH})} \quad (2)$$

To implement the model, NMR spectra were acquired for each sample matrix (i.e. clover, whole soil, fine clay, coarse clay, fine silt, and (clover + uracil + soil)) with systematic variation of the contact and delay times. Model parameters were generated with either the COMPLEX nonlinear optimization program of Box (Kuester and Mize, 1973; as modified by Dr. Thomas Manetsch, Michigan State University) or the Marquardt method within PROC NLIN of the SAS software (SAS Institute, 1989); standard errors of the parameters were computed using SAS.

2.4. Clover-N mineralization in whole soil and particle-size fractions

Clover-N mineralization in whole soil and particle-size fractions was measured by the kinetic analysis of organic clover-derived N in whole soils and particle-size fractions as a function of incubation time. The clover-derived N amounts in the various fractions were computed with the assumption that isotopic discrimination

Table 2
Summary of ^{15}N chemical shifts

Shift region (ppm)	Nitrogen functionality
0	Ammonium
5–34	Amino groups in free and amino-terminal amino acids
42–76	Amino groups of nucleic acids, guanidine nitrogens of arginine, indole-N of tryptophan
83–116	Amide N of proteins
120–148	Heterocyclic N in certain positions in nucleic acids, in histidine, or in flavin
158	Heterocyclic N in pyrrole (chlorophyll)
170–211	Heterocyclic N in nucleic acids, in flavin, or in pyrrole (chlorophyll)
312–320	Heterocyclic N in oxidized flavin structures
354	Nitrate

was negligible, and the data were fit to one of two mathematical models.

The first model was a two-pool exponential decay:

$$N_t = N_1 \exp(-k_1 t) + N_2 \exp(-k_2 t) \quad (3)$$

where N_t is the amount of N at time $= t$, N_1 and N_2 are the N amounts in the pools at the beginning of incubation, and k_1 and k_2 are rate constants.

The second model was applicable in the fine and coarse clay fractions, where a period of net N accumulation preceded a period of net N depletion:

$$N_t = -A \exp(-k_A t) + B \exp(-k_D t) \quad (4)$$

where A and B are (positive) constants, k_A is the accumulation rate constant, and k_D is the depletion rate constant.

Parameter estimates and standard errors in the models were generated via the Levenberg–Marquardt method within the nonlinear regression module (PROC NLIN) of the SAS software (SAS Institute, 1989).

3. Results and discussion

3.1. NMR quantitation test

The ^{15}N- CPMAS–NMR spectrum of the prepared mixture of (^{15}N-clover + ^{15}N-uracil + unlabeled soil) is shown in Fig. 3. The two N atoms of uracil are evident as well as the amide, guanidinium, and amino N functional groups of clover. Severe peak overlap is evident among the uracil and amide nitrogens. The peak area percentages were initially obtained by integrating the NMR signal between the limits of the observed peaks, with and without correction for differential relaxation (columns 2 and 3 of Table 3). Differential relaxation effects were small for the sample because (1) the delay time for the spectrum of Fig. 3 (1.25 s) was substantially greater than the maximum value of T_{1H} (0.454 s, data not shown), and (2) the correction factors for differential relaxation during the contact time [Eq. (2)] were approximately equal for all functional groups (data not shown). With or without correction for differential relaxation, the NMR peak area percentages did not correspond to the known sample composition (Table 3, column 1). Peak overlap was considered a likely source of this error.

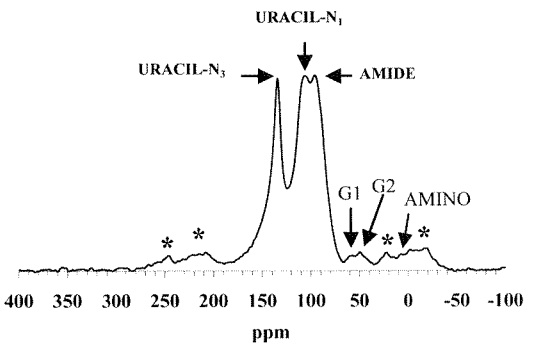

Fig. 3. ^{15}N-NMR spectrum of prepared sample of ^{15}N-uracil + ^{15}N-clover + unlabeled soil. Contact time = 0.2 ms, delay time = 1.25 s. G1 = guanidinium –NH- of arginine, G2 = guanidinium –NH2 of arginine, * = spinning sideband.

Assuming that the lack of agreement between the known sample composition and the peak area percentages as obtained by integrating the NMR signal between the observed peaks resulted from peak overlap among the uracil and amide peaks, the "true" contributions of uracil-N_1, uracil-N_3, and clover were calculated by modeling the (^{15}N-clover + ^{15}N-uracil + unlabeled soil) spectrum as a linear combination of the simpler spectra acquired for (^{15}N-clover + unlabeled soil) and (^{15}N-uracil + unlabeled soil). The modeled and measured (^{15}N-clover + ^{15}N-uracil + unlabeled soil) spectra were not significantly different, and the peak area percentages as determined by the model closely matched the known sample composition (Table 3, column 4- see Appendix B for details). Although the peak modeling described here is likely not practical for samples of unknown composition, the modeling confirms that the signal of each functional group in the spectrum of Fig. 3 is proportional to the number of N atoms in each group and that all ^{15}N in the (^{15}N-clover + ^{15}N-uracil + soil) system was detectable. The practical conclusion is that, in the absence of peak overlap, ^{15}N-CPMAS–NMR was quantitative for a soil sample containing a complex mixture of noncyclic N and protonated heterocyclic N.

3.2. Clover-N mineralization in incubated soils

The dynamics of clover-N in the whole soil and size fractions are described reasonably well by simple kinetic models (Fig. 4). The data are based on isotope dilution equations, with the assumption that isotopic fractionation is negligible. Further, the data have been adjusted for (1) loss of soil mass during particle-size separation (mass loss $\leqslant 9\%$), (2) incomplete dispersion on day 11 of the incubation due to failure to hand-shake the soil plus added water prior to sonication (fine and coarse clay yields were 35 and 64% of expected, respectively), and (3) variability in clay recovery. These adjustments entailed normalization of the clover-N amounts in the particle-size fractions in accord with expected particle-size yields. (See Appendix C for particle-size recovery data.)

Sand- and coarse silt-associated clover-N were characterized primarily by a fast-decaying organic N pool ($k = 0.12$–0.16 day^{-1}), which likely represented large plant fragments (*macroorganic matter*) in the early stages of decomposition. The presence of such fragments was verified by direct visual observation or

Table 3
Test of quantitative ^{15}N-NMR in prepared mixture of (^{15}N-uracil + ^{15}N-clover + unlabeled soil)

^{15}N form	1. Known sample composition (percentage of total N)[b]	2. ^{15}N-NMR peak area percentages (uncorrected)[c,d]	3. ^{15}N-NMR peak area percentages (corrected for differential relaxation)[d,e]	4. ^{15}N-NMR peak area percentages (corrected for differential relaxation and peak overlap)[f]
Uracil-N_3[a]	25 (1)	33	34	22
Uracil-N_1[a]	25 (1)	30	30	25
Clover (*Trifolium pratense* L.)	50 (4)	37	35	53

[a] Subscripts refer to ring position of ^{15}N.

[b] Computed from ^{15}N concentrations in clover and uracil. Clover ^{15}N concentration was determined by mass spectrometer; uracil ^{15}N concentrations were provided by manufacturer; soil ^{15}N concentration was negligible. Sample standard deviations (in parentheses) were computed based on uncertainty in masses, ^{15}N concentration, and moisture contents of the mixture components.

[c] One NMR spectrum was acquired. The estimated uncertainties in peak area percentages due to phasing, baseline correction, and spectral noise were less than 0.5% of total signal intensity.

[d] Peak area percentages were determined by integrating the spectrum of Fig. 3 according to the observed peak regions. Peaks were integrated with the following limits (ppm): uracil-N_3, 281–240, 178–123, 31–12; uracil-N_1, 240–216, 123–101, 1––12; amide, 216–198, 101–64,−12 to −60; guanidinium, 64–31; amino, 12 to −1.

[e] Differential relaxation effects corrected per Eq. (1).

[f] Peak overlap corrections based on linear combination of (uracil + soil) and (clover + soil) spectra as described in text and Appendix B.

microscopy (50×). The fine silt contained two clover-N pools; the faster pool had an intermediate decay rate ($k = 0.03$ day^{-1}) and probably was macroorganic matter (with entrapped mineral particles) in an intermediate stage of decomposition. The slow pool within the fine silt ($k = 0.001$ day^{-1}) is attributed to sorbed N. The clay fractions exhibited fast accumulation ($k = 0.04$–0.07 day^{-1}) followed by slow depletion ($k = 0.001$ day^{-1}) of clover-N, and were modeled with the assumption that both processes followed an exponential trend [Eq. (4)]. The accumulation is considered a result of the microbially mediated transfer of N from coarser fractions, and the depletion reflects the slow mineralization of clay-sorbed N. The transient presence of N in coarse fractions and the stabilization of N in fine fractions is consistent with the field studies of Aita et al. (1997) and Balabane and Balesdent (1995), and conforms to current concepts of organic nutrient flow in soils (e.g. Christensen, 1996).

The decay rate constants for the clay-associated clover-N and for the slow-decaying pool of fine silt-associated clover-N (approximately 0.001 day^{-1}) correspond to a mean residence time (MRT) of 3 years in the laboratory, or 7 years in the field. This field MRT was calculated by adjusting for temperature differences between the laboratory and local Michigan field conditions ($Q_{10} = 2$; Kätterer et al., 1998). No attempt was made to account for variations in moisture that would be expected in the field, as moisture was not correlated with CO_2 fluxes in a field study in southwest Michigan (Paul et al., 1999).

The agronomic relevance of the medium- to long-term stabilization of clover-N observed here (i.e. MRT = 7 years in fine particle-size fractions) can be assessed by comparing the overall retention of added plant-N in this study to that observed in the field by others (Table 4). The overall retention of added N in the present study closely matches that of Aita et al. (1997), but is greater than that observed by Harris and Hesterman (1990). The higher decomposition (lower retention) observed by Harris and Hesterman (1990) could be a result of the presence of growing plants (Cortez and Cherqui, 1991), differences in the amount of substrate added, or textural effects. This analysis suggests that some but not all field mechanisms of N mineralization and immobilization were operating in the present study.

3.3. NMR spectroscopy of clover and incubated clover-amended soils

The CPMAS–NMR spectra of clover, whole soil, fine clay, coarse clay, and fine silt are shown in Figs. 5 and 6. (No spectra were acquired for the coarse silt and sand fractions due to the low concentrations of ^{15}N in these fractions.) The peak area percentages (corrected for differential relaxation effects) are summarized in Table 5. Throughout the incubation, the ^{15}N functional group composition of the whole soil and size fractions was not significantly different from that of pure clover; the organic N was approximately 85–90% amide, 5–10% guanidinium N of arginine, and 5% amino. No significant amount of heterocyclic N was detected.

The spectrum of pure clover (Fig. 5) is better resolved than the spectra of the soil samples and can be viewed as representative of organic clover-derived N throughout the incubation. The strong amide signal (95 ppm) suggests that the clover-N is mostly proteinaceous; therefore, the other peaks in the spectrum probably represent non-amide N within amino acids. The small peak at 150 ppm is likely to be the heterocyclic N of histidine.

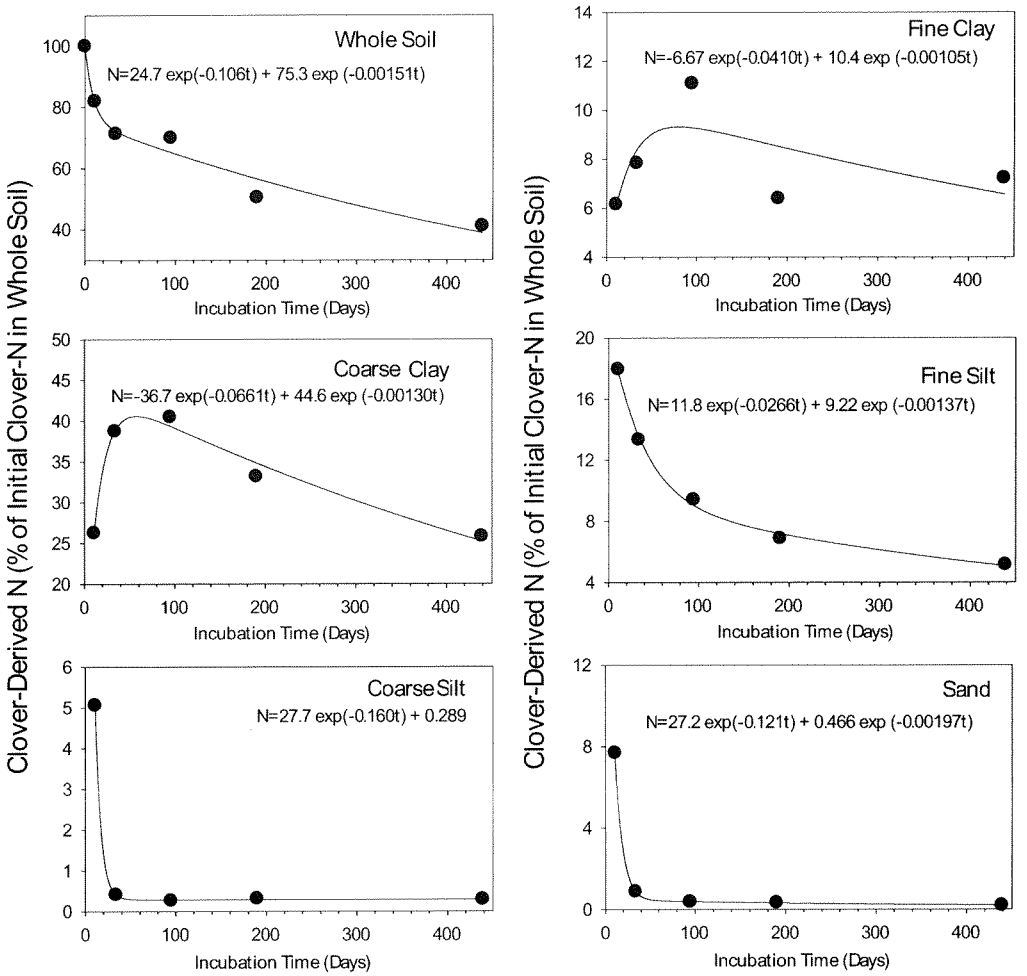

Fig. 4. Clover-derived N amounts in incubated soil (measured ●, modelled —).

Table 4
^{15}N retention in present study compared to field studies

Agronomic system	Field studies		Present study
	Decomposition conditions	Added ^{15}N remaining as percentage of initial	Added ^{15}N remaining as percentage of initial[a]
^{15}N-wheat straw decomposition in absence of growing plants[b]	365 days, 10 °C, 45 kg straw-N per ha, silt loam soil	59	60
^{15}N-alfalfa decomposition in presence of corn[c]	332 days, 10 °C, 112 kg alfalfa-N per ha, sandy loam soil	40	61

[a] Corrected to time and temperature of field studies.
[b] Aita et al., 1997.
[c] Harris and Hesterman, 1990.

Stoichiometric considerations strongly suggest that the peaks at 58 and 45 ppm are the –NH– and $-NH_2$ units of the guanidinium group of arginine, respectively. The ratio of the relaxation-corrected peak areas (–NH–: $-NH_2$ = 1:2.5, data not shown) was close to the expected stoichiometric value (1:2) for the guanidinium group. The two peaks in the region −10 to 20 ppm probably represent the amino groups of free or amino-terminal amino acids (Table 2 and Appendix A).

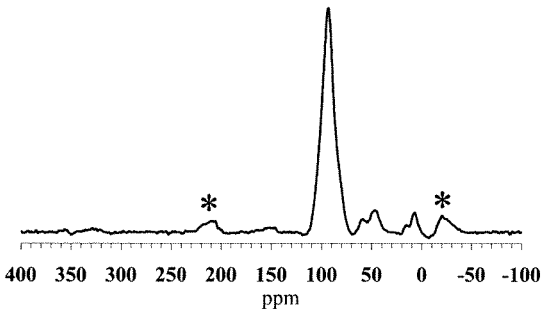

Fig. 5. ^{15}N-NMR spectrum of clover. Contact time = 0.4 ms, delay time = 1 s. * = spinning sideband.

The overall corrections for differential relaxation effects were small in the spectra of clover and incubated soils; the maximum difference between corrected and uncorrected peak area percentages for each sample corresponded to no more than 3% of the total signal intensity. The relaxation model of Eq. (1) fitted the data well, as evidenced by the generally low ratios of standard errors to relaxation parameter values (Table 6). The poorer fits for the amino group relative to other functional groups are likely a result of the relatively small peak area of the amino group as well as peak overlap (Figs. 5 and 6). The correction factors for differential relaxation during the contact time were computed from T_{NH} and $T_{1\rho H}$ [Eq. (2), Table 7]. Within each sample, the ratio of the maximum to the minimum correction factor among the various functional groups varied from about 1 to 1.5. (A high maximum:minimum ratio indicates that differential relaxation effects during the contact time may be significant.) The highest correction factor usually corresponded to the amino group, probably as a result of high T_{NH} values for the amino group (Table 6). High T_{NH} values are expected in relatively mobile functional groups such as the amino group (Kinchesh et al., 1995).

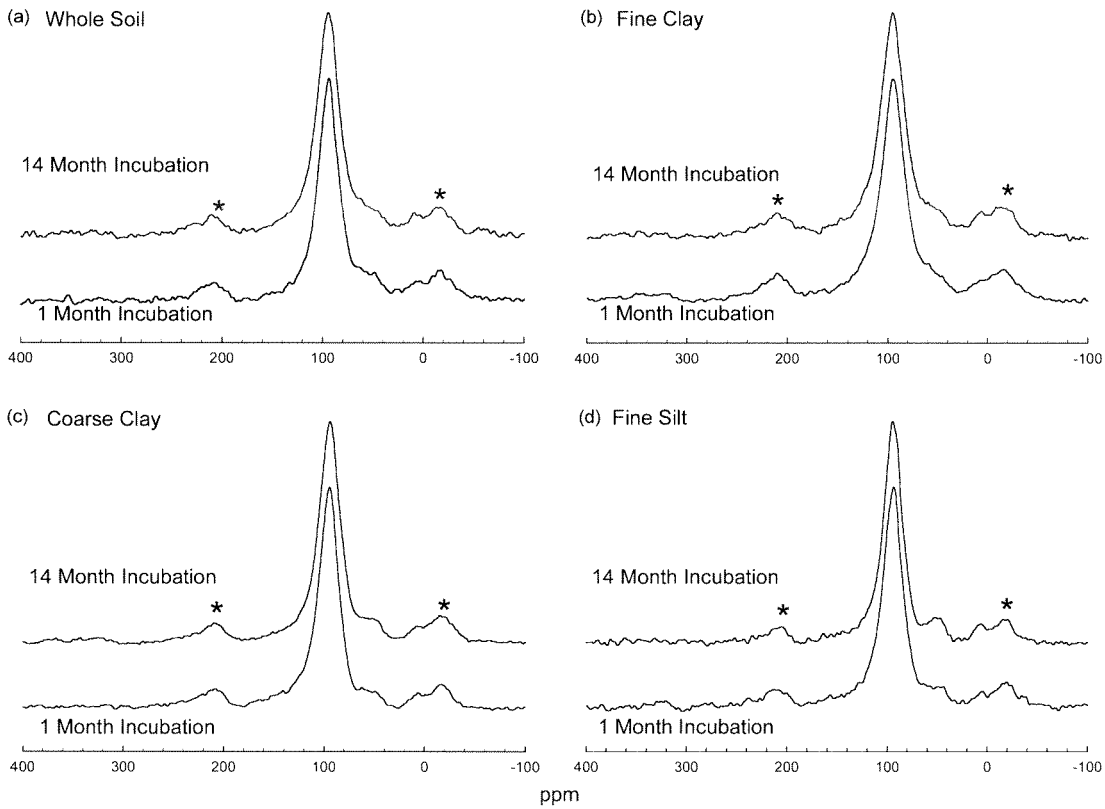

Fig. 6. ^{15}N-NMR spectra of (a) whole soil, (b) fine clay, (c) coarse clay, (d) fine silt. Contact time = 0.4 ms (all samples), delay time = 0.5 s (whole soil, fine clay), 0.9 s (coarse clay, 1 month), 1 s (coarse clay, 14 month), 0.75 s (fine silt). * = spinning sideband.

Table 5
NMR peak area percentages for clover and incubated soil[a,b,c]

Material→	Clover	Whole soil			Fine clay			Coarse clay			Fine silt		
Incubation time (d)→	0	34	190	439	34	190	439	34	190	439	34	190	439
Aromatic N of histidine	1	0	0	0	0	0	0	0	0	0	0	0	0
Amide	85	85	86	85	86	84	86	92	91	90	89	87	88
Guanidinium N's of arginine	8	8	8	9	8	9	8	6	6	7	7	8	7
amino	6	7	6	7	6	7	6	3	3	3	3	5	4

[a] Each data point is based on one (unreplicated) spectrum. Each spectrum underwent data processing twice (Fourier transformation + phasing + baseline correction), and final peak areas were calculated as the means of the two peak areas.

[b] Due to peak overlap, spectral noise, and subjectivity in phasing and baseline correction, differences of less than 5–10% of total signal intensity are probably not significant.

[c] Data have been corrected for differential relaxation per Eq. (1). These corrections altered the peak area percentages by no more than 3% of total signal intensity.

The linear correlation of the NMR spectral intensities with the amounts of ^{15}N in the incubated soil samples supports the quantitative accuracy of CPMAS–NMR (Fig. 7). Linear regressions were run with ^{15}N amount (from mass spectrometric analysis) and total NMR signal intensity per scan as dependent and independent variables, respectively. Regressions were run separately for each soil fraction using only spectra that had been collected in a single NMR session; thus, confounding effects due to soil fraction (e.g. differential Fe contents) and variation in spectrometer performance were avoided. The correlations for whole soil, fine clay, coarse clay, and fine silt were all significant ($P \leqslant 0.05$), and the regression lines for each fraction passed extremely close to the origin (Fig. 7). If some N (e.g. nonprotonated heterocycles, see Kelemen et al., 2002) was inherently undetectable, the regression lines would be expected to intercept the vertical axes in Fig. 7 well above the origin. The lowest R^2 value for NMR spectral intensity versus ^{15}N concentration was obtained for fine clay, and a plot of detectability (NMR signal intensity per scan per μmol ^{15}N) versus incubation time revealed an apparent decrease in the detectability of ^{15}N with increasing incubation time (Fig. 8). If it is assumed that the ^{15}N is 100% detectable at day 34, Fig. 8 indicates that about 30% of the fine-clay ^{15}N may have been undetectable at day 439. This decrease in detectability suggests that a form of undetectable N, such as nonprotonated heterocyclic N or heterocyclic N in slow-relaxing rigid aromatic structures (or perhaps clay-sorbed NH_4), may have slowly formed in the fine clay. This undetectable ^{15}N corresponded to about 5% of the remaining ^{15}N in the whole soil. Overall, the regressions suggest that most of the ^{15}N was detected by NMR over the 14-month time course of this study.

The above analysis of NMR data suggests that very little, if any, heterocyclic ^{15}N was formed during the soil incubation. It is possible that the broad high-frequency (left-hand) shoulder of the amide peak observed here (Fig. 6) and in other studies (e.g. Knicker et al., 1993; Knicker and Lüdemann, 1995) may be a result of heterocyclic N. However, comparison of the spectra of ^{15}N-clover in the presence and absence of soil (Fig. 9) suggests that the shoulder is simply a consequence of soil-induced line broadening (due perhaps to soil iron) rather than peak overlap between amide-N and a potentially obscured heterocyclic N group. The shoulder does obscure a small heterocyclic N signal due to histidine (near 150 ppm), but this signal represents only about 1% of the clover-^{15}N (Table 5).

3.4. Chemical structure of soil organic N as determined by NMR: a critical analysis

The quantitativeness of NMR was supported through successful characterization of differential relaxation effects, analysis of a complex soil-organic mixture with known composition, and strong correlation of NMR spectral intensities with ^{15}N concentrations as measured on a mass spectrometer. The relatively small differential relaxation effects observed here should not be generalized; samples that contain appreciable amounts of both high-mobility N (e.g. amino) and limited-mobility N (e.g. amide) would be expected to exhibit relatively large differential relaxation effects. The analysis of the (^{15}N-clover + ^{15}N-uracil + unlabeled soil) mixture of known composition showed that peak overlap is an important though not fatal weakness of the NMR analysis of soil samples. Nevertheless, peak overlap did not appear significant in any of the incubated (^{15}N-clover + soil) samples—the peak area of each functional group was accurate to within about 5% of the total spectral intensity.

The composition of ^{15}N in whole soils and particle-size fractions in this study (85–90% amide, 5–10% guanidinium N of arginine, and 5% amino) is in good agreement with other ^{15}N-CPMAS–NMR studies of soil but at variance with the composition of soil N as proposed by Schulten and Schnitzer (1998). The composi-

Table 6
T_{1H}, T_{NH}, and $T_{1\rho H}$ values for clover and incubated soils[a]

Material	Functional group					
	Aromatic N of histidine	Amide	Guanidinium N's of arginine		Amino	
			–NH	$-NH_2$		
T_{1H} (s)						
Clover[b]	0.37	0.53	NA[c]	0.52	0.97	0.83
	(0.43)	(0.10)		(0.10)	(1.56)	(0.08)
Whole soil	ND[d]	0.19	NA		0.52	
		(0.01)			(0.17)	
Fine clay	ND	0.14	NA		NA	
		(0.05)				
Coarse clay	ND	0.20	NA		NA	
		(0.05)				
Fine silt	ND	0.18	NA		0.21	
		(0.02)			(0.06)	
T_{NH} (ms)						
Clover[b]	0.13	0.059	0.050	0.060	0.061	0.29
	(0.05)	(0.009)	(0.018)	(0.006)	(0.058)	(0.10)
Whole soil	ND	0.078	0.089		0.19	
		(0.008)	(0.009)		(0.04)	
Fine clay	ND	0.076	0.085		0.16	
		(0.009)	(0.022)		(0.10)	
Coarse clay	ND	0.062	0.055		0.13	
		(0.004)	(0.022)		(0.06)	
Fine silt	ND	0.072	0.082		0.27	
		(0.005)	(0.011)		(0.08)	
$T_{1\rho H}$ (ms)						
Clover[b]	3.15	2.14	1.96	1.41	12.6	1.65
	(1.48)	(0.28)	(0.58)	(0.11)	(29.3)	(0.59)
Whole soil	ND	3.24	1.95		1.95	
		(0.33)	(0.19)		(0.46)	
Fine clay	ND	2.15	1.67		0.93	
		(0.23)	(0.40)		(0.56)	
Coarse clay	ND	2.29	1.80		2.83	
		(0.12)	(0.60)		(1.42)	
Fine silt	ND	3.17	2.19		2.60	
		(0.24)	(0.28)		(0.88)	

[a] Standard error in parentheses. For the incubated soils, model parameters were generated only for samples that had been incubated for 34 days. The parameters were assumed to be equally applicable to soils that had been incubated for different times.

[b] For clover, two peaks were observed in both the guanidinium and amino regions. Values on the left correspond to the peaks with the higher NMR frequency.

[c] NA = no dependence of signal intensity upon delay time was observed; functional group assumed to be fully relaxed. Minimum delay values tested were as follows: 1 s (clover), 0.5 s (whole soil, fine clay, coarse clay, and fine silt).

[d] ND = functional group not detected.

tion of soil N per Schulten and Schnitzer is: proteins + peptides + amino acids, 40%; amino sugars, 5–6%; heterocyclic N, 35%; and NH_3, 19%. (NH_3 is an operationally defined pool; see Introduction.) Schulten and Schnitzer (1998) argue that the incubation times of ^{15}N-amended soils in studies such as the present one may be too short for the formation (or selective preservation) of resistant heterocyclic N. While the long-term formation of heterocyclic N could not be evaluated from the data of the present study, kinetic analysis indicated that the clover-N in this study had a mean residence time of 3 years in the laboratory, which corresponded to approximately 7 years in the field. This material thus seems to have at least medium-term stability.

The discrepancy in N chemical composition between NMR-based studies and the study of Schulten and Schnitzer (1998) may stem from the assumptions used by Schulten and Schnitzer. Their analysis appears to

rely on the assumption that no proteinaceous N is contained in the N fraction that is resistant to hot acid hydrolysis (Sowden et al., 1977). This assumption may be reasonable in some studies, as hot acid hydrolysis is a traditional method for decomposing proteins into their constituent amino acids (Creighton, 1993). However, ^{15}N-CPMAS–NMR analysis of the nonhydrolyzable residue of a soil incubated for 2 years with ^{15}N-ammonium sulfate + crop residues + powdered filter paper revealed that about 80% of the N in the residue was in the form of amide and amino groups; about 20% could be assigned to either amide or heterocyclic N of indole (Zhuo et al., 1992). Similarly, the ^{15}N-NMR analysis (at natural abundance levels) of the hydrolysis residue from an organic-rich lake sediment produced an amide-dominated spectrum quite similar to the spectra acquired in the present study (Knicker and Hatcher, 1997). Further analysis of the residue (thermochemolysis followed by gas chromatography/mass spectrometry) identified the N as proteinaceous (Knicker and Hatcher, 1997).

Table 7
Contact-time correction factors[a]

Material	Functional group						Max. correction factor / Min. correction factor
	Imidazole N of histidine[b]	Amide	Guanidinium N's of arginine		Amino		
			–NH	–NH_2			
Clover[c]	1.146	1.174	1.196	1.274	1.029	1.551	1.51
Whole soil	–	1.112	1.188		1.298		1.17
Fine clay	–	1.169	1.220		1.459		1.25
Coarse clay	–	1.161	1.212		1.161		1.04
Fine silt	–	1.114	1.166		1.418		1.27

[a] Contact-time correction factor defined in Eq. (2). For the incubated soils, model parameters were generated only for samples that had been incubated for 34 days. The parameters were assumed to be equally applicable to soils that had been incubated for different times.

[b] Imidazole N was observed in clover only.

[c] For clover, two peaks were observed in both the guanidinium and amino regions. Values on the left correspond to the peaks with the higher NMR frequency.

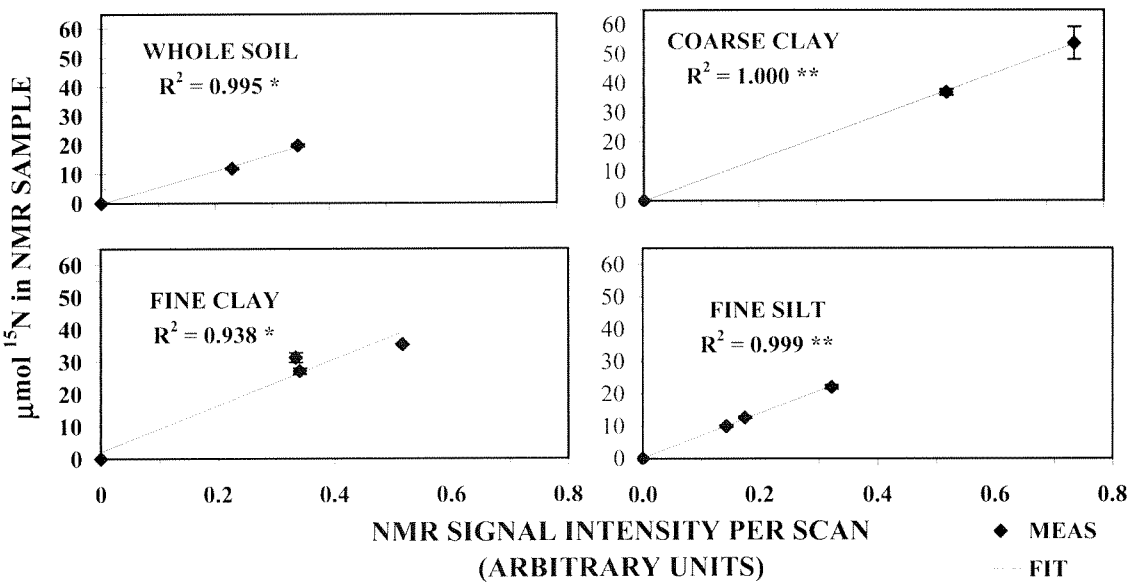

Fig. 7. Linear regressions of ^{15}N amounts versus NMR signal intensity for soil samples. Each point represents a soil sample collected after 1, 6, or 14 months of incubation. The point (0,0) is not a measured point, but was included in the input data for the regressions since no signal would be expected for a blank sample. Because each regression was restricted to spectra collected in a single experimental session, the number of points in each regression varies. Error bars represent sample standard deviations from mass spectrometric measurement of ^{15}N. * and ** indicate significance at the 0.05 and 0.01 probability levels, respectively.

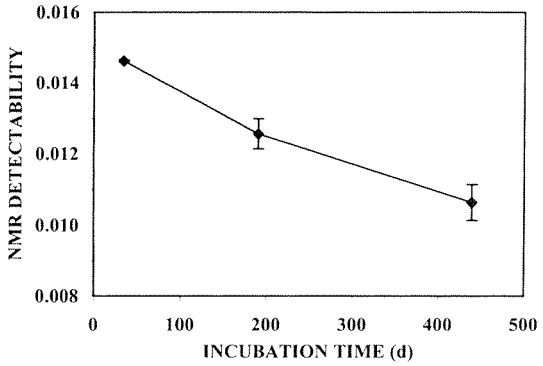

Fig. 8. NMR detectability of fine-clay associated ^{15}N after various incubation times. NMR detectability is defined as NMR signal intensity per scan per μmol ^{15}N.

Additionally, Zang et al. (2000) combined ^{15}N-labeled protein extracts with humic acids and found that a significant portion of the protein in this mixture was resistant to acid hydrolysis.

Based on the unchanging proteinaceous NMR signature of clover-derived N throughout the 14-month soil incubation, the considerable differences in the mineralization/immobilization behavior of clover-N among the different particle-size fractions appear not to be linked with chemical functional group. Possible mechanisms for the stability of proteinaceous N in the fine soil fractions of this study include adsorption onto clays, entrapment of soil N in pores inaccessible to microbes, or humification without change of functional group (e.g. cross-linking of large biomolecules or encapsulation of proteinaceous material by other biomolecules).

Improvements in ^{15}N-NMR spectroscopy of soils seem possible, but not without conceptual or technical challenges. Density fractionation leads to isolation of fractions low in specific gravity and relatively high in organic content; such schemes were used in a ^{13}C-NMR study by Baldock et al. (1992). However, Christensen (1992) has questioned some density fractionation schemes, and considers that density fractions of clay and silt particles may not represent truly distinct pools of organic matter. Dissolution of mineral matter by HF may improve NMR spectra (Schmidt et al., 1997), but this approach would seem to forfeit the advantage of the noninvasiveness of NMR. Finally, the recently developed technique of high-resolution solid-state ^{14}N-NMR may help resolve the current controversy surrounding the chemical structure of native soil organic N (Jeschke and Jansen, 1998). However, this approach requires high spinning speeds and further advances in broadband spectral excitation, and may not be immediately applicable to soil systems.

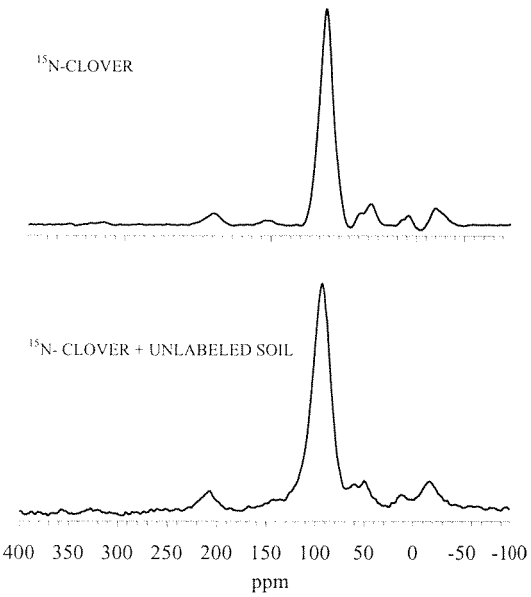

Fig. 9. NMR spectra of ^{15}N-labeled clover, with and without soil. In both spectra, contact time = 0.2 ms, delay = 1 s, line broadening = 120 Hz.

Acknowledgements

This material is based upon work supported by the Cooperative State Research Service, US Department of Agriculture, under Agreement No. 94-37107-0387. Any opinions, findings, conclusions, or recommendations expressed in this publication are those of the authors and do not necessarily reflect the view of the US Department of Agriculture. The senior author is grateful for the financial support of the US Department of Agriculture (Water Sciences Fellowship) and the Michigan State University Department of Crop and Soil Sciences (Graduate Office Fellowship). We thank Dr. Karl Bishop, Dr. Utami DiCosty, Dr. Boyd Ellis, Mr. Jason Franti, Dr. Dave Harris, Mr. Kermit Johnson, Ms. Pat Outcalt, Mr. Bryan Pape, and Dr. Oliver Schabenberger for invaluable technical assistance, and we thank three anonymous reviewers for helping to improve the manuscript.

Associate Editor—**Klaus Schmidt-Rohr**

Appendix A. Detailed table of ^{15}N chemical shifts

^{15}N chemical shifts of biologically important molecules

Compound	Chemical shift (ppm)	Ref.[a]
Ammonium sulfate or ^{15}N-ammonium ^{14}N-nitrate	0	–
Free amino acids, amino groups	5–34 (including Gly and Pro)	5
Guanidine–NH2	42–53	1,5
Guanidine–NH-	60–65	
–NH2 of nucleic acids	76 (C); 59 (A); 53 (G)	2
Tryptophan–NH–(indole)	61	1
Peptide-N	83–116 (including Gly and Pro) 95–110 (excluding Gly and Pro)	1,5
Uracil[b]	111 (N1), 139 (N3)	1
Histidine ring N (imidazole)	145–155 cation; 157 & 211 amphiion; 173 & 197 anion	1
Aromatic N in nucleic acids[c]		
G3, T3, C1, G1, T1	121–140	2
A9, G9	148	2
C3, A3, A1, A7, G7	174–211	2
Pyrrole	136 (in DMSO-d_6)	4
Pyrrole as part of chlorophyll A	173, 175, 192, 233 (in acetone-d_6)	1
Flavin (isoalloxazine)	128–140 (N3); 142 (N10, ox.); 170–179 (N1); 312-320 (N5, ox.)	1
Nitrate	354	3

[a]1. Blomberg and Ruterjans, 1983; 2. Cross et al., 1982; 3. Levy and Lichter, 1979; 4. Thorn and Mikita, 1992; 5. Wuthrich, 1976. [b]Hawkes et al., 1977; as cited by Blomberg and Ruterjans (1983). [c]A = adenine, C = cytosine, G = guanine, T = thymine.

Appendix B. Computation of "true" contributions of uracil and clover to NMR signal intensity in the severely overlapped ^{15}N-NMR spectrum of (^{15}N-clover + ^{15}N-uracil + unlabeled soil)

The "true" contributions of uracil-N_1, uracil-N_3, and clover-N to the NMR spectrum of (^{15}N-clover + ^{15}N-uracil + unlabeled soil) (Fig. 3) were calculated by modeling the spectrum as a linear combination of the simpler spectra acquired for (^{15}N-clover + unlabeled soil) and (^{15}N-uracil + unlabeled soil). This was accomplished as shown below:

Mathematically, at each NMR frequency ν in the spectrum, the measured intensity, $S_{CUS,MEAS}(\nu)$ is modeled as:

$$S_{CUS,MODEL}(\nu) = k_{US}S_{US,MEAS}(\nu) + k_{CS}S_{CS,MEAS}(\nu) \quad (2.1)$$

where $S_{US,MEAS}(\nu)$ and $S_{CS,MEAS}(\nu)$ are the measured signals in the (^{15}N-uracil + unlabeled soil) and (^{15}N-clover + unlabeled soil) spectra, respectively, and k_{US} and k_{CS} are positive constants. The constants k_{US} and k_{CS} were determined by least-squares minimization of χ^2:

$$\frac{\sum_{\nu=\nu_L}^{\nu_R}\left(S_{CUS,MEAS}(\nu) - S_{CUS,MODEL}(\nu)\right)^2}{\left(VAR_{CUS,MEAS} + VAR_{CUS,MODEL}\right)f} \quad (2.2)$$

where ν_L and ν_R are the NMR frequencies of the left and right edges of the spectral region of interest, f is the degrees of freedom (f = number of NMR frequencies in spectral region of interest minus two), $VAR_{CUS,MEAS}$ is the variance of the measured spectrum of (^{15}N-clover + ^{15}N-uracil + unlabeled soil) and $VAR_{CUS,MODEL}$ is the variance of the modeled spectrum of (^{15}N-clover + ^{15}N-uracil + unlabeled soil). According to Bevington and Robinson (1992), a sufficiently small value of χ^2 indicates that the two distributions in the numerator of Eq. (2.2) are not significantly different.

The variance of the measured spectrum in Eq. (2.2) was estimated as the variance in signal intensity in 25 points chosen from a portion of the spectrum without peaks. The variance of the modeled spectrum was based on the rules of statistical error propagation:

$$VAR_{CUS,MODEL} = k_{US}^2 VAR_{US,MEAS} + k_{CS}^2 VAR_{CS,MEAS} \quad (2.3)$$

where k_{US} and k_{CS} are the constants from Eq. (2.1), and $VAR_{US,MEAS}$ and $VAR_{CS,MEAS}$ are the variances of the measured spectra of (^{15}N-uracil + unlabeled soil) and (^{15}N-clover + unlabeled soil). $VAR_{US,MEAS}$ and $VAR_{CS,MEAS}$ were computed per the aforementioned 25-point method.

The chi-square minimization of Eq. (2.2) yielded $\chi^2 = 49.41$, corresponding to $P = 1.000$; thus the simulated and measured spectra (not shown) were not significantly different. Therefore, the modeled spectrum was considered statistically valid and the "true" peak area percentages of the (^{15}N-clover + ^{15}N-uracil + unlabeled soil) sample were calculated as:

$$PAP_{U-N3} = \frac{k_{US} PA_{U-N3,US}}{PA_{TOTAL}} \times 100$$

$$PAP_{U-N1} = \frac{k_{US} PA_{U-N1,US}}{PA_{TOTAL}} \times 100$$

$$PAP_{CLOV} = \frac{k_{CS} PA_{CLOV,CS}}{PA_{TOTAL}} \times 100$$

where PAP_{U-N3} and PAP_{U-N1} are peak area percentages in the modeled (^{15}N-clover + ^{15}N-uracil + unlabeled soil) spectrum due to uracil N at ring positions 3 and 1, respectively. $PA_{U-N3,US}$ and $PA_{U-N1,US}$ are peak areas of uracil-N_3 and uracil-N_1 in the measured (^{15}N-uracil + unlabeled soil) spectrum, respectively, and were calculated by integrating the NMR signal of said spectrum between the observed peak limits. PAP_{CLOV} is the peak area percentage in the modeled spectrum due to clover, and $PA_{CLOV,CS}$ is the (total) peak area in the measured (^{15}N-clover + unlabeled soil) spectrum. PA_{TOTAL} is defined as: $PA_{TOTAL} = k_{US}(PA_{U-N3,US} + PA_{U-N1,US}) + k_{CS}\, PA_{CLOV,CS}$

Appendix C. Recovery of mass in ultrasonic particle-size fractionations[a]

Fraction	Expected distribution[b]	Incubation time (days)				
		11	34	95	190	439
Fine clay (<0.2 μm)	3.8±0.6	1.3	3.6	4.3	3.2	4.2
Coarse clay (0.2–2 μm)	12.4±0.7	7.9	12.1	12.1	13.4	12.1
Fine silt (2–10 μm)	12.0±0.4	13.8	12.4	12.1	11.9	11.6
Coarse silt (10–53 μm)	15.4±2.9	16.2	17.0	16.8	16.9	17.9
Sand (53–2000 μm)	56.3±3.1	60.8	54.9	54.7	54.7	54.1
Recovery (%)[c]	–	93	93	93	91	93

[a]Data are percent of recovered mass, unless otherwise noted. [b]Means and sample standard deviations from preliminary study as described in Materials and Methods and Table 1. [c]Recovery (%) = 100×soil mass recovered in all fractions/unfractionated soil mass.

References

Aita, C., Recous, S., Angers, D.A., 1997. Short-term kinetics of residual wheat straw C and N under field conditions: characterization by $^{13}C^{15}N$ tracing and soil particle size fractionation. European Journal of Soil Science 48, 283–294.

Balabane, M., Balesdent, J., 1995. Medium-term transformations of organic N in a cultivated soil. European Journal of Soil Science 46, 497–505.

Baldock, J.A., Oades, J.M., Waters, A.G., Peng, X., Vassallo, A.M., Wilson, M.A., 1992. Aspects of the chemical structure of soil organic materials as revealed by solid-state ^{13}C NMR spectroscopy. Biogeochemistry 16, 1–42.

Bevington, P.R., Robinson, D.K., 1992. Data Reduction and Error Analysis for the Physical Sciences, second ed. McGraw-Hill, New York.

Bliss, C.I., 1967. Statistics in Biology, Vol. 1. McGraw-Hill, New York.

Blomberg, F., Ruterjans, H., 1983. Nitrogen-15 NMR in biological systems. In: Berliner, L.J., Reuben, J. (Eds.), Biological Magnetic Resonance, Vol. 5. Plenum Press, New York, pp. 21–73.

Brady, N.C., 1990. The Nature and Properties of Soils, tenth ed. Macmillan Publishing Company, New York.

Catroux, G., Schnitzer, M., 1987. Chemical, spectroscopic, and biological characteristics of the organic matter in particle size fractions separated from an Aquoll. Soil Science Society of America Journal 51, 1200–1207.

Christensen, B.T., 1992. Physical fractionation of soil and organic matter in primary particle size and density separates. In: Stewart, B.A. (Ed.), Advances in Soil Science, Vol. 20. Springer-Verlag, New York, pp. 1–90.

Christensen, B.T., 1996. Matching measurable soil organic matter fractions with conceptual pools in simulation models of carbon turnover: revision of model structure. In: Powlson, D.S., Smith, P., Smith, J.U. (Eds.), Evaluation of Soil Organic Matter Models Using Existing Long-Term Datasets, 1996. (Eds.), NATO ASI Series I 38. Springer-Verlag, Berlin, pp. 143–159.

Clinton, P.W., Newman, R.H., Allen, R.B., 1995. Immobilization of ^{15}N in forest litter studied by ^{15}N CPMAS NMR spectroscopy. European Journal of Soil Science 46, 551–556.

Cortez, J., Cherqui, A., 1991. Plant growth and the mineralization of adsorbed ^{14}C- and ^{15}N-labelled compounds. Soil Biology and Biochemistry 23, 261–267.

Creighton, T.E., 1993. Proteins: Structures and Molecular Properties, second ed. WH Freeman and Company, New York.

Cross, T.A., DiVerdi, J.A., Opella, S.J., 1982. Strategy for nitrogen NMR of biopolymers. Journal of the American Chemical Society 104, 1759–1761.

Elonen, P., 1971. Particle-size analysis of soil. Acta Agralia Fennica 122.

Gee, G.W., Bauder, J.W., 1986. Particle-size analysis. In: Klute, A. (Ed.), Methods of Soil Analysis, Part 1. Physical and Mineralogical Methods, second ed, 1986. (Ed.), Agronomy Monograph 9. American Society of Agronomy—Soil Science Society of America, Madison, WI, pp. 383–411.

Harris, G.H., Hesterman, O.B., 1990. Quantifying the nitrogen contribution from alfalfa to soil and two succeeding crops using nitrogen-15. Agronomy Journal 82, 129–134.

Hopkins, D.W., Chudek, J.A., Webster, E.A., Barraclough, D., 1997. Following the decomposition of ryegrass labelled with ^{13}C and ^{15}N in soil by solid-state nuclear magnetic resonance spectroscopy. European Journal of Soil Science 48, 623–631.

Jeschke, G., Jansen, M., 1998. High-resolution 14N solid-state NMR spectroscopy. Angewandte Chemie International Edition 37, 1282–1283.

Kätterer, T., Reichstein, M., Andrén, O., Lomander, A., 1998. Temperature dependence of organic matter decomposition: a critical review using literature data analyzed with different models. Biology and Fertility of Soils 27, 258–262.

Kelemen, S.R., Afeworki, M., Gorbaty, M.L., Kwiatek, P.J., Solum, M.S., Hu, J.Z., Pugmire, R.J., 2002. XPS and ^{15}N NMR study of nitrogen forms in carbonaceous solids. Energy and Fuels 16, 1507–1515.

Kinchesh, P., Powlson, D.S., Randall, E.W., 1995. ^{13}C NMR studies of organic matter in whole soils: I. Quantitation possibilities. European Journal of Soil Science 46, 125–138.

Knicker, H., Fründ, R., Lüdemann, H.-D., 1993. The chemical nature of nitrogen in native soil organic matter. Die Naturwissenschaften 80, 219–221.

Knicker, H., Lüdemann, H.-D., 1995. N-15 and C-13 CPMAS and solution NMR studies of N-15 enriched plant material during 600 days of microbial degradation. Organic Geochemistry 23, 329–341.

Knicker, H., Hatcher, P.G., 1997. Survival of protein in an organic-rich sediment: possible protection by encapsulation in organic matter. Die Naturwissenschaften 84, 231–234.

Knicker, H., Rüdiger, F., Lüdemann, H.-D., 1997. Characterization of nitrogen in plant composts and native humic material by natural-abundance 15N CPMAS and solution NMR spectra. In: Nanny, M.A., Minear, R.A., Leenheer, J.A. (Eds.), Nuclear Magnetic Resonance Spectroscopy in Environmental Chemistry. Oxford University Press, New York, pp. 272–294.

Knicker, H., Schmidt, M.W.I., Kögel-Knabner, I., 1999. The structure of organic nitrogen in particle size fractions determined by ^{15}N CPMAS NMR. In: Berthelin, J., Huang, P.M., Bollag, J.-M., Andreux, F. (Eds.), Effect of Mineral-Organic-Microorganism Interactions on Soil and Freshwater Environments. , pp. 143–149.

Kuester, J.L., Mize, J.H., 1973. Optimization Techniques with FORTRAN. McGraw-Hill, New York.

Levy, G.C., Lichter, R.L., 1979. Nitrogen-15 Nuclear Magnetic Resonance Spectroscopy. John Wiley & Sons, New York.

Mahieu, N., Olk, D.C., Randall, E.W., 2000. Accumulation of heterocyclic nitrogen in humified organic matter: a 15N-NMR study of lowland rice soils. European Journal of Soil Science 51, 379–389.

Morra, M.J., Blank, R.R., Freeborn, L.L., Shafii, B., 1991. Size fractionation of soil organo-mineral complexes using ultrasonic dispersion. Soil Science 152, 294–303.

Nadelhoffer, K.J., 1990. Microlysimeter for measuring nitrogen mineralization and microbial respiration in aerobic soil incubations. Soil Science Society of America Journal 54, 411–415.

North, P.F., 1976. Towards an absolute measurement of soil structural stability using ultrasound. Journal of Soil Science 27, 451–459.

Paul, E.A., Harris, D., Collins, H.P., Schulthess, U., Robertson, G.P., 1999. Evolution of CO2 and soil carbon dynamics in biologically managed, row-crop agroecosystems. Applied Soil Ecology 11, 53–65.

SAS Institute Inc, 1989. SAS/STAT User's Guide, Version 6, Volume 2, fouth ed. SAS Institute Inc, Cary, NC.

Schmidt, M.W.I., Knicker, H., Hatcher, P.G., Kögel-Knabner, I., 1997. Improvement of ^{13}C and ^{15}N CPMAS NMR spectra of bulk soils, particle-size fractions and organic material by treatment with 10% hydrofluoric acid. European Journal of Soil Science 48, 319–328.

Schnitzer, M., 1985. Nature of nitrogen in humic substances. In: Aiken, G.R., McKnight, D.M., Wershaw, R.L., MacCarthy, P. (Eds.), Humic Substances in Soil, Sediment, and Water: Geochemistry, Isolation, and Characterization. John Wiley and Sons, New York, pp. 303–325.

Schulten, H.-R., Hempfling, R., 1992. Influence of agricultural soil management on humus composition and dynamics: classical and modern analytical techniques. Plant and Soil 142, 259–271.

Schulten, H.-R., Sorge, C., Schnitzer, M., 1995. Structural studies on soil nitrogen by Curie-point pyrolysis-gas chromatography/mass spectrometry with nitrogen-selective detection. Biology and Fertility of Soils 20, 174–184.

Schulten, H.-R., Schnitzer, M., 1998. The chemistry of soil organic nitrogen: a review. Biology and Fertility of Soils 26, 1–15.

Sowden, F.J., Chen, Y., Schnitzer, M., 1977. The nitrogen distribution in soils formed under widely varying climatic conditions. Geochimica et Cosmochimica Acta 41, 1524–1526.

Stejskal, E.O., Memory, J.D., 1994. High Resolution NMR in the Solid State. Oxford University Press, New York.

Stevenson, F.J., 1994. Humus Chemistry: Genesis, Composition, Reactions, second ed. John Wiley and Sons, New York.

Thorn, K.A., Mikita, M.A., 1992. Ammonia fixation by humic substances: a nitrogen-15 and carbon-13 NMR study. Science of the Total Environment 113, 67–87.

Whittig, L.D., Allardice, W.R., 1986. X-ray diffraction techniques. In: Klute, A. (Ed.), Methods of Soil Analysis, Part 1. Physical and Mineralogical Methods. American Society of Agronomy—Soil Science Society of America, Madison, WI, pp. 331–362.

Wilson, M.A., Vassallo, A.M., Collin, P.J., Rottendorf, H., 1984. High-resolution carbon-13 nuclear magnetic resonance spectroscopy and relaxation behavior of organic solids from fossil fuels. Analytical Chemistry 56, 433–436.

Wuthrich, K., 1976. NMR in Biological Research: Peptides and Proteins. North Holland/American Elsevier, Amsterdam/New York.

Zang, X., van Heemst, J.D.H., Dria, K.J., Hatcher, P.G., 2000. Encapsulation of protein in humic acid from a histosol as an explanation for the occurrence of organic nitrogen in soil and sediment. Organic Geochemistry 31, 679–695.

Zhuo, S.-N., Wen, Q.-X., 1992. Nitrogen forms in humic substances. Pedosphere 2, 307–315.

Zhuo, S.-N., Wen, Q.-X., Du, L.-J., Wu, S.-L., 1992. The nitrogen form of nonhydrolyzable residue of humic acid. Chinese Science Bulletin 37, 508–511.